from accumulating within the putative intracellular compartment. Phlorizin, acting at the mucosal border inhibits the uptake of sugars across the mucosal entry pathway, but does not affect 2-deoxy-galactose, or galactose movement via the alternative pathway, hence does not affect active secretion, indeed it may enhance it. This investigation was supported by a travel grant from the Royal Society (London) and a Dahlgren Fellowship from MDIBL to R.J. Naftalin, as well as by a grant from the Whitehall Foundation to A. Kleinzeller.

MICROVASCULAR ORGANIZATION OF THE GILL OF *S. acanthias*

Kenneth R. Olson, Michael Levy, Steven Falchuk and Barbara Kent, South Bend Center for Medical Education, Indiana University School of Medicine. Notre Dame University, Notre Dame, Indiana; Mount Sinai School of Medicine, New York, New York; and Veterans Administration Medical Center, Bronx, New York

Physiological studies of pressure-flow relationships in the gill of *S. acanthias* demonstrate a marked increase in resistance to flow within the gill vasculature in response to various stimuli such as hypoxia and hypercapnia (Kent and Peirce, Comp. Biochem. Physiol. 60(C):37-44, 1978). Recent studies using thermal washout techniques suggest that the vasomotion may include A-V shunting (Eid et al., Bull. MDIBL 17:91-94, 1977). Anatomic evidence for such shunts is lacking (Kempton, Biol. Bull. 136: 226-240, 1969); indeed the literature on the microvasculature of the gill of dogfish is quite sparse. Recently techniques utilizing vascular casting and SEM studies have proved fruitful in detailing the gill vasculature in teleosts (Olson et al., Fed. Proc. 37:387, 1978). In the present studies these techniques have been applied to the dogfish.

Four dogfish ranging in weight from 4 to 6 kg were anesthetized with sodium pentobarbital (20 mg/kg), heparinized via the caudal artery (1000 units/kg) and placed in a seawater trough ventral side up. Fresh seawater from tubes in the spiracles ran over the gills. The conus arteriosus was cannulated with a short, large bore cannula (PE270) through which dogfish Ringer's (Robin) was pumped at a pressure similar to ventral aortic pressure (40-50 mmHg). The atrium was opened and Ringer's was allowed to run through the vasculature of the fish for at least 10 minutes or until red cells were completely washed out. A plexiglass resin and catalyst (Mercox) was pumped in following the Ringer's at the same pressure for 10 minutes. Excess Mercox escaped from the open atrium when the circulatory system was completely filled. The fish were transferred to a 50°C water bath for an hour and the gill basket was removed and put in a 20 % NaOH solution where tissue was digested. The Mercox cast of the gills was then rinsed with distilled water and air dried.

Specimens were examined microscopically with a Wilde M5 microscope at the South Bend extension of Indiana University Medical School and with a Cambridge Stereoscan 600 scanning electron microscope at the Notre Dame University Biology Department.

The distribution of the afferent branchial artery in the first hemibranch is seen in Figure 1. In Figure 1 primary filamental afferent arteries (16 shown) leave the afferent branchial artery and distribute to the mid-portion of either one or two filaments. Here the vessel bifurcates into a recurrent branch running to the basal end of the filament and a concurrent branch which supplies the filament to the outer tip. Along the entire length of the filament both the recurrent and concurrent filamental afferent arteries give rise to lateral and medial afferent sinuses. These join with those of adjacent filaments along the outer margin of the hemibranch as seen in Figure 1. This figure also shows that the distal end of the concurrent filamental afferent artery divides and becomes indistinguishable from the sinuses at the outer margin. Figure 2 shows a detail of the lateral view of the medial afferent sinus as it comes off the filamental afferent artery. Part of the lateral sinus has been removed from this section of the artery. The afferent lamellar arterioles can be seen arising from the

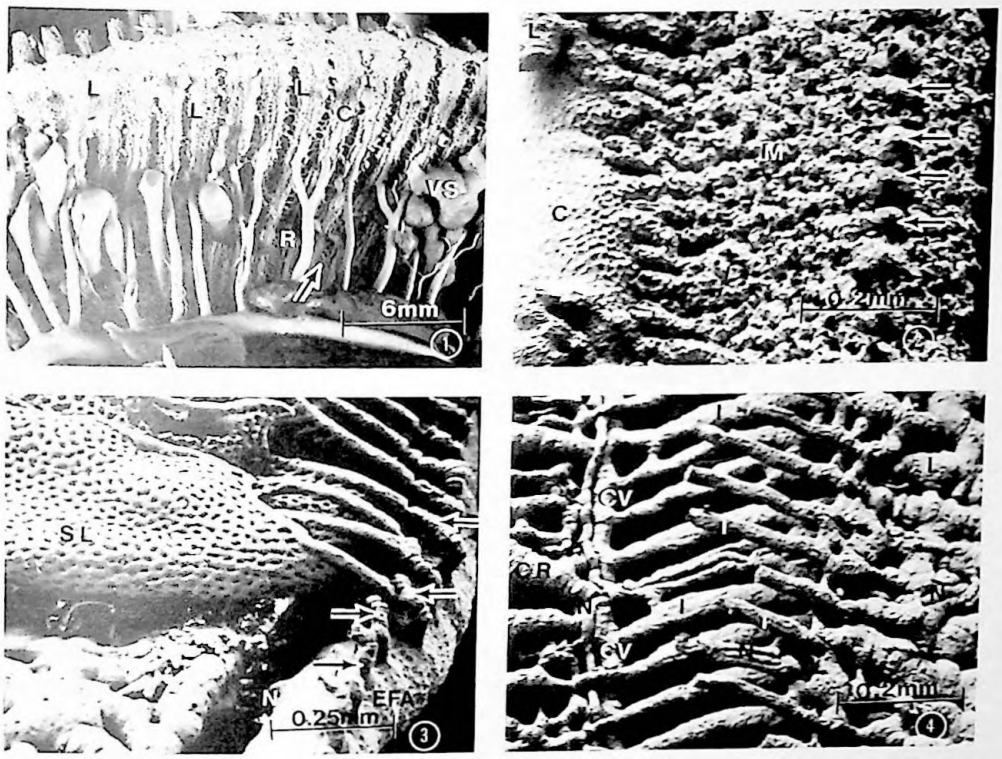

Figure 1. Light micrograph of afferent vasculature of 1st hemibranch, x2.5 ↑collateral reticulum.
Figure 2. SEM of medial afferent sinus, x75 ↑afferent lamellar arterioles
Figure 3. SEM of efferent lamellar arterioles, x60 ↑efferent lamellar arteriole
Figure 4. SEM detail of collateral circulation, x75

Key to Figures 1-6

C, concurrent afferent filamental artery
CR, collateral reticulum
CV, collateral vessel
EFA, efferent filamental artery
I, interlamellar vessels
L, lateral afferent sinus
M, medial afferent sinus
N, nutritive vessel
O, outer marginal channel
R, recurrent afferent filamental artery
SL, secondary lamellae
VS, collateral sinus
W, water channel

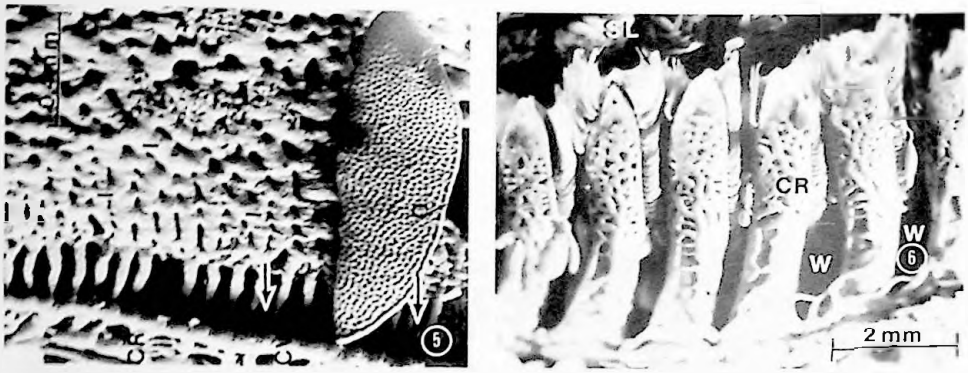

Figure 5. SEM of afferent lamellar arterioles interdigitating with interlamellar vessels, x37.5
* afferent lamellar arterioles
Figure 6. Light micrograph of outer end of filaments, x7.5

network of the medial sinus. The secondary lamellae have been removed so that several afferent lamellar arterioles may be seen in a row. The efferent lamellar attachment may be seen in Figure 3. Here several secondary lamellae can be seen attaching by way of the efferent lamellar arterioles directly into the efferent filamental artery. In the foreground, lower right, of Figure 3 is a row of efferent lamellar arterioles from which the lamellae have been removed. A nutritive vessel (N) may be seen leaving the efferent filamental artery (EFA).

Coincident with but independent of the filamental vasculature thus far described is a second, collateral circulation. Collateral vessels run in parallel the length of the filament on each side of the afferent filamental artery and are connected between adjacent filaments by a collateral reticulum (see Figures 1, 4 and 5). The collateral vessels give rise to interlamellar vessels which run parallel to the lamellar intermarginal channel and extend vertically from the surface of the filament (Figure 4). The interlamellar vessels leave the collateral vessels via a series of short, straight parallel channels (Figure 4) which run across the medial sinus from each side of the filament. The interlamellar vessels (arrows, Figure 5) interdigitate with the short afferent lamellar arterioles. In Figure 5 most of the lamellae have been removed to show the afferent lamellar arterioles protruding out between the columns of interlamellar vessels. One lamella is still attached so that its position may be seen relative to the interlamellar vessels. The outer marginal channel of this lamella may be seen clearly. There is no connection between the lamellae and the interlamellar vessels, nor is there continuity between the interlamellar vessels and the efferent filamental artery. At the distal tip of the filament the two collateral vessels of a single filament join to form a fenestrated saddle which covers the end of the medial sinus (Figure 6). Extensions of the collateral vessels go beyond the margin of the hemibranch into the opercular skin. The collateral reticulum between filaments provides the blood supply to the tissue at the base of the water channels. The flow of blood through the respiratory or lamellar part of the microvasculature is traced in diagramatic form in Figure 7 by the heavy lines. As might be expected from the low resistance nature of the respiratory circuit there are many possible pathways leading to the lamellae. Blood in one afferent filamental artery probably proceeds to its own medial afferent sinus but could flow on to adjacent filaments through lateral afferent sinuses at the tip of the filament. The direction of flow within the medial afferent sinus is not altogether clear but from the interconnecting nature of the channel undoubtedly blood could pass from one side of the filament to the

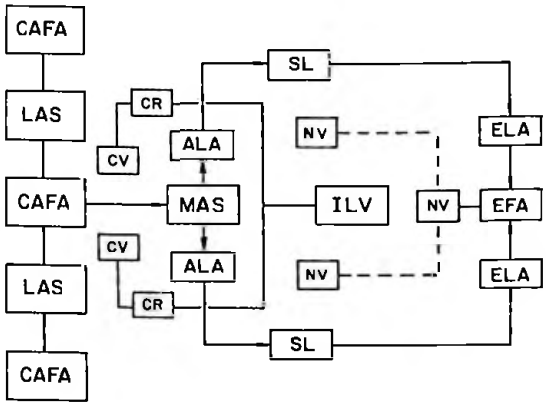

ALA Afferent lamellar arteriole
CAFA Concurrent afferent filamental artery
CR Collateral reticulum
CV Collateral vessel
EFA Efferent filamental artery
ELA Efferent lamellar arteriole
ILV Interlamellar vessels
LAS Lateral afferent sinus
MAS Medial afferent sinus
NV Nutritive vessel
SL Secondary lamella

Figure 7. Block diagram of gill vascular organization

other or up and down to continue into any one of the afferent lamellar arterioles. Within the lamellae the course the blood takes seems to be limited to either through the maze of pillar cells or around the inner or outer marginal channels. Once through the lamellae with the exception of flow through nutritive vessels blood flows in an uninterrupted course via efferent lamellar arterioles and efferent filamental arteries back into the systemic circuit.

There are several locations within this scheme which seem to be prime sites for control of resistance and hence gill blood flow. Constriction or dilation of portions of the filamental artery would, of course, preferentially channel blood into different filamental sections of lamellae. A more interesting possible site of resistance change is in the afferent lamellar arteriole. This vessel is virtually yoked by the interlamellar vessels of the collateral circulation (Figure 7). A pressure change in the collateral system might modulate tissue pressure surrounding the afferent lamellar arteriole and hence transmural pressure to effect significant changes in the resistance to flow through the afferent lamellar arteriole. In this way, a separate circulation and one possibly linked to the osmoregulatory functions of the gill would become a controller of the blood flow pattern in the respiratory part of the gill circulation. A third site of resistance change is in the efferent lamellar arteriole. Several of our micrographs illustrate constrictions in this arteriole before it joins the efferent filamental artery. There are also constrictions of the efferent filamental artery between lamellar arteriolar junctions.

There are several features of the dogfish circulation shown by the corrosion casting technique which were heretofore unobserved. Kempton, using classic histological tissue slice techniques, described a "cavernous body" between the afferent filamental artery and the afferent lamellar arterioles. With the casting technique this structure is shown to be a sinus which not only branches laterally as well as medially from the afferent filamental arteries, but also connects the blood supply of all the filaments. Kempton also mentions "septal vessels" and makes note of the paucity of red cells contained in them. We have chosen to rename these the interlamellar vessels since they are analogous to structures in the collateral circulation of teleost gills where nomenclature is better established. The origin of the collateral circulation is uncertain in teleosts and we could not identify a beginning point in elasmobranchs. There is the possibility that the collateral circulation is fed by valved lymphatics which would not be filled by Mercox under the conditions of this study. The extensive filling of the collateral circulation would have to be from the venous side. There is good evidence that the collateral circulation drains into large venous vessels running in the septum. The collateral reticulum is continuous with structures designated as collateral sinus in Figure 1. The lack of red cells found in interlamellar vessels is consistent with the idea of a lymphatic origin. Another interesting aspect

of the collateral circulation is its proximity at the base of the filament to cells described by Doyle (Bull. MDIBL · 15:27-28, 1975) as analogous to teleost chloride cells. Perhaps the collateral circulation is an inter-gill lymphatic venous system designed to aid in osmoregulation.

Although many interesting new aspects of the dogfish gill microvasculature were found, there was no evidence of an anatomic A-V shunt of the respiratory lamellae. Perhaps the anatomic basis for physiological shunting lies in the lamellae themselves. Preferential flow through the outer margins may influence gas exchange characteristics, or simply thickening of the blood layer within the lamella might result in a difference in gas exchange and a change in physiological shunt. This work was supported by Research Project #4901-01 and 02. Veterans Administration Medical Center, Bronx, New York, and by NSF grant PCM 76-16840.

PLATINATE INHIBITION OF WINTER FLOUNDER (*Pseudopleuronectes americanus*) RENAL TUBULAR FUNCTION

David S. Miller, Susan T. Arnold, Linda A. Butler, Jussi Melartin and Anthony M. Guarino
Mount Desert Island Biological Laboratory, Salsbury Cove, Maine, and National Cancer Institute, National Institute of Health, Bethesda, Maryland

Thirty years ago, Forster suggested that the isolated flounder tubule preparation could provide a rapid screening test for agents that modify tubular secretion (Science 108:65-67, 1948). Since then, this preparation has been used to correlate tubular dysfunction with histopathological lesions after exposure to nephrotoxins and to study subcellular sites of drug and pollutant toxicity (J. Exp. Zool. 199:365-382, 1977; Miller, unpublished data). We present here data which indicate that this preparation could be useful in assessing platinate nephrotoxicity. cis-Dichlorodiamineplatinum (II) (cisPt) and certain analogues have been shown to possess antitumor activity in animal test systems. In the search for new analogues with a higher therapeutic index, nearly 1000 platinates have emerged. Since, testing all of these drugs for nephrotoxicity in whole animal systems would be prohibitively expensive, a rapid in vitro screening test could aid in selecting the most promising for further study.

TABLE 1

Inhibition of renal tubular PAH transport and Na,K-ATPase activity by platinates *

NSC No.	Brief Name	I_{50} Flounder PAH Uptake	I_{50} Flounder ATPase	I_{50} Rat ATPase
4958	$PtCl_3$	0.01	0.001	0.06
119,875	cis Pt	0.8	5.0	2
131,558	trans Pt	0.5	-	-
224,964	cyclohexanediamine propanediato Pt	0.15	1.0	-
247,541	Discreet	1.0	-	-
250,427	cyclohexanediamine sulfato	0.1	0.2	0.5
256,927	di Cl di OH propanamine	2.5	0.5	-
263,158	cyclohexanediamine methanesulfanato	0.05	0.005	0.04
267,583	diammine guanosine di Cl	4.0	-	-
268,252	cyclohexanediamine di OH	0.25	-	-
271,674	cyclohexanediamine benzene tricarboxylato	0.2	0.1	-

* I_{50} values (the concentration of inhibitor causing 50% inhibition) calculated from plot of % inhibition vs. log platinate concentration. Transport data reflects inhibition of active component only; thus, 1.0 was subtracted from both control and experimental T/M values before calculation of % inhibition. Na,K-ATPase data generated by addition of drug to enzyme assay medium.

Flounder kidneys were teased into 20 mg batches of tubules and each bath was preincubated in 5 ml of Forster's marine teleost buffer (FB); containing 140 mM NaCl, 2.5 mM KCl, 1 mM $MgCl_2$, 7.5 mM $NaHCO_3$, 0.5 mM NaH_2PO_4, 0.5 mM $CaCl_2$, at pH 8.25, with or without (control) 0.001-10 mM drug. After 0.24 hr, 0.5 ml of FB containing both ^{14}C and unlabeled p-aminohippuric acid (PAH) was added to each vial; the final PAH concentration was 10 µM. After a 45 min incubation with PAH, tissues in each vial were divided into two 10 mg samples and each sample was weighed, solubilized and counted. Both incubation and preincubation were carried out at 17°C under 100% O_2. With control tissue, 45-min incubations yielded steady state values for PAH uptake and thus reflected the ability of the tubules to concentrate organic anions. Control uptakes were nearly constant after 0-6 hr preincubations, with uncorrected tissue to medium ratios (T/M) averaging